Journal of Experimental Botany Advance Access published April 18, 2015

Journal of Experimental Botany
doi:10.1093/jxb/erv110

RESEARCH PAPER

Low concentrations of the toxin ophiobolin A lead to an arrest of the cell cycle and alter the intracellular partitioning of glutathione between the nuclei and cytoplasm

Vittoria Locato[1], Esther Novo Uzal[1,2], Sara Cimini[1], Maria Chiara Zonno[3], Antonio Evidente[4], Alessandra Micera[5], Christine H. Foyer[6] and Laura De Gara[1,*]

[1] Centro Integrato di Ricerca, Università Campus Bio-Medico, Via Alvaro del Portillo, 00128 Roma, Italy
[2] Departamento de Biología Vegetal, Universidad de Murcia, Campus Espinardo, Murcia, Spain
[3] Istituto di Scienze delle Produzioni Alimentari, Consiglio Nazionale delle Ricerche, Via Amendola 122/O, 70125 Bari, Italy
[4] Dipartimento di Scienze Chimiche, Università di Napoli Federico II, Complesso Universitario Monte S. Angelo, Via Cinthia 4, 80126 Napoli; Italy
[5] IRCCS-G.B. Fondazione Bietti, Roma, Italy
[6] Centre for Plant Sciences, Faculty of Biology, University of Leeds, Leeds LS2 9JT, UK

* To whom correspondence should be addressed. E-mail: l.degara@unicampus.it

Received 28 November 2014; Revised 4 February 2015; Accepted 18 February 2015

Abstract

Ophiobolin A, a tetracyclic sesterpenoid produced by phytopathogenic fungi, is responsible for catastrophic losses in crop yield but its mechanism of action is not understood. The effects of ophiobolin A were therefore investigated on the growth and redox metabolism of Tobacco Bright Yellow-2 (TBY-2) cell cultures by applying concentrations of the toxin that did not promote cell death. At concentrations between 2–5 μM, ophiobolin A inhibited growth and proliferation of the TBY-2 cells, which remained viable. Microscopic and cytofluorimetric analyses showed that ophiobolin A treatment caused a rapid decrease in mitotic index, with a lower percentage of the cells at G1 and increased numbers of cells at the S/G2 phases. Cell size was not changed following treatment suggesting that the arrest of cell cycle progression was not the result of a block on cell growth. The characteristic glutathione redox state and the localization of glutathione in the nucleus during cell proliferation were not changed by ophiobolin A. However, subsequent decreases in glutathione and the re-distribution of glutathione between the cytoplasm and nuclei after mitosis occurring in control cells, as well as the profile of glutathionylated proteins, were changed in the presence of the toxin. The profile of poly ADP-ribosylated proteins were also modified by ophiobolin A. Taken together, these data provide evidence of the mechanism of ophiobolin A action as a cell cycle inhibitor and further demonstrate the link between nuclear glutathione and the cell cycle regulation, suggesting that glutathione-dependent redox controls in the nuclei prior to cell division are of pivotal importance.

Key words: Cell cycle, glutathione, glutathionylation, ophiobolin A, poly-ADP-ribosylation, Tobacco Bright Yellow-2.

Introduction

Ophiobolins are sesterpenoids produced by phytopathogenic fungi, mostly of the *Bipolaris, Aspergillus*, and *Drechslera* genera. These fungi attack several monocot crops such as rice (*Oryza sativa* L.), maize (*Zea mays* L.), and sorghum (*Sorghum* ssp.) and have been the cause of catastrophic losses of cereal yield all over the world (Au *et al.*, 2000). Currently,

25 biogenic analogues of ophiobolins have been identified. Ophiobolin A (see Supplementary Fig. S1 at *JXB* online) was the first member of the group to be isolated and characterized in the mid-1960s (Nozoe *et al.*, 1965; Canonica *et al.*, 1966). This toxin can adversely affect cell proliferation in mammalian cells at very low concentrations, even in lines which are resistant to pro-apoptotic stimuli, an effect that is of increasing interest particularly with regard to target pathways (Bury *et al.*, 2013).

Although ophiobolins are considered to be responsible for the injuries caused by the fungi on susceptible plants (mainly monocotyledons), their mode of action is not understood (Au *et al.*, 2000). An interaction between ophiobolin and a maize calmodulin *in vitro* has been reported (Leung et al., 1984, 1985). Ophiobolin A also induces programmed cell death (PCD) in Tobacco Bright Yellow-2 (TBY2) cultured cells (Bury *et al.*, 2013). Tobacco is able to activate defence responses against ophiobolin-producing fungi, consistent with the fact that these fungi are mainly pathogenic in monocots and not in dicots (Au *et al.*, 2000). Moreover, sub-lethal concentrations of ophiobolin A inhibit the growth of cell cultures without affecting viability (Bury *et al.*, 2013).

The regulation of the cellular redox state has been reported to be a crucial factor controlling cell growth in plants as it is in animal systems (Pellny *et al.*, 2009; Foyer and Noctor, 2009; Chiu and Dawes, 2012; de Pinto *et al.*, 2012). Cell cycle progression in eukaryotes is considered to be driven by an intrinsic redox cycle consisting of reductive and oxidative phases (Chiu and Dawes, 2012). In animals, a mild oxidative environment is able to activate a signalling pathway leading to cell proliferation (Menon *et al.*, 2003; Menon and Goswami, 2007). The interaction between growth factors, such as EGF and their specific receptors stimulate cell proliferation by the generation of low amounts of ROS (Menon and Goswami, 2007). Sensing the redox environment is important so that cell cycle progression can occur under appropriate redox conditions. Indeed, many regulatory proteins in the cell cycle have been found to be redox sensitive (Chiu and Dawes, 2012). Protein and non- protein thiols appear to undergo an oxidative cycle during the G1 and S phases. The first evidence of this type of cell cycle regulation dates backs almost 50 years ago, when non protein-thiols were found to decrease during G1 and to increase again during S phase (Mauro *et al.*, 1969).

Links between the cellular redox state and the cell cycle have been suggested by studies on the root quiescent centre, where stem cells reside in a largely oxidized environment (Jiang and Feldman, 2005; Jiang *et al.*, 2006; Dinneny *et al.*, 2008). While the regulation of the cell cycle by fluctuations in the cellular redox state have not been described in plants, reduced glutathione (GSH), which is the most abundant cellular non-protein thiol, is localized in the nucleus during the early stages of the cell cycle (Markovic *et al.*, 2009; Pellny *et al.*, 2009; Vivancos *et al.*, 2010). In the nucleus, GSH provides the reductive environment required to protect DNA against oxidation during replication (Garcia- Gimenez et al., 2013). Depletion of the nuclear GSH pool disrupts cell proliferation (Markovic *et al.*, 2009). The following experiments were undertaken in order to determine whether sub-lethal ophiobolin A concentrations altered the redox and glutathione homeostasis of Tobacco Bright Yellow-2 (TBY-2) cells growing in culture, in relation to effects on the cell cycle. Microscopic analyses and cytofluorimetric assays show that ophiobolin A leads to an arrest of the cell cycle, alters the partitioning of GSH between the nuclei and cytosol, and modifies redox-related protein modifications.

Materials and methods

Ophiobolin A production and purification

Ophiobolin A was extracted from *Drechslera gigantea* (Heald & Wolf) culture filtrates and purified as previously described (Evidente *et al.*, 2006). The ophiobolin A purity (>95%) was confirmed by RP-HPLC-UV. HPLC analyses were performed on an Agilent 1100 series HPLC system (Agilent, Diegem, Belgium). The chromatographic system was a C8 SunFire 150 × 4.6 mm I.D., 3.5 µm particle size (Waters, Milford, MA, USA). The solvents were CH_3OH:TFA 0.1 % in water (65:35 by vol.), with a flow rate of 0.75 ml min^{-1} and λ=240 nm. The purity was further confirmed by ^1H NMR and ESI MS spectroscopic investigation carried out in $CDCl_3$ at 400/100 MHz in $CDCl_3$ on Bruker spectrometers and Agilent Technologies 6120 Quadrupole LC/MS instruments, respectively.

TBY-2 cell culture growth conditions and ophiobolin A treatments

The suspension of tobacco (*Nicotiana tabacum* L. cv. Bright-Yellow 2) cells was routinely propagated and cultured at 27 °C according to Nagata *et al.* (1992). A stationary culture was diluted 4:100 (v/v) and cultured in a new medium (Nagata *et al.*, 1992).

After 2 d of growth of the new established cell culture, ophiobolin A was re-suspended in ethanol and filtered into the cell suspension. The amount of ethanol never exceeded 0.2% of the total volume.

Cell culture growth was followed over time by measuring optical density at 600 nm (Pellny *et al.*, 2009). Cell length was determined by white light microscopy using the Scion Image software.

Mitotic index

The mitotic index was calculated as the percentage of the ratio between dividing cells and the number of cells scored. For each time analysed, at least 300 cells were observed. The number of dividing cells was determined by Hoechst 33258 staining as reported in Houot *et al.* (2001), and visualized using a fluorescence microscope (DMLS, Leica, Wetzlar, Germany) with an excitation filter of 340–380 nm and a barrier filter of 410 nm.

Cell cycle analysis by flow cytofluorimetry

Cell cycle phases were determined by the estimation of the DNA content in TBY-2 cell nuclei using propidium iodide (50 µg ml^{-1}; PI) staining and flow cytometry analysis (Fried *et al.*, 1976).

In order to isolate TBY-2 cell nuclei, protoplasts have be obtained as mainly described in Locato *et al.* (2009). Briefly, 1 g of control and ophiobolin A-treated cells was re-suspended in 4 ml protoplast extraction buffer (0.4 M mannitol, 25 mM TRIS-MES, pH 5.5 with HCl, with 0.25% (w/v) cellulose (Sigma, C1794), 0.05% (w/v) pectolyase (Sigma, P5936), 0.1% (v/v) pectinase (Sigma, P4716) added on the day). The cells were incubated in the dark with gentle agitation for about 90 min to obtain protoplasts. Progress was monitored by observing sub-samples of the cells under the light microscope. Protoplasts were recovered by centrifugation at 200 *g* for 5 min at room temperature without using the brake. The pellet was washed twice with the protoplast washing buffer (0.4 M mannitol, 25 mM TRIS-MES, pH 6.5 with HCl) in the same centrifugation conditions.

Nuclei were isolated using the Cell-Lytic P Kit (Sigma-Aldrich, St Louis, MA, USA) following the manufacturer's instructions. Protoplasts have been re-suspended in 2 ml NIBA (Nuclear Isolation Buffer with 1% (v/v) Protease Inhibitor Cocktail and 1 mM DTT). Following this step, every operation was performed on ice. Protoplasts were disrupted using a Dounce homogenizer, with six strokes with the loose followed by 6–9 strokes with the tight- fitting pestle. Progress was monitored using the light microscope. Aliquots of the lysate have been put through a vacuum filtration on four layers of Miracloth paper. Two millilitres of the filtrate were washed twice with TBS (20 mM TRIS, 137 mM NaCl, pH 7.6) by centrifugation at 1500 *g* for 10 min at 4 °C without using the brake. After the second washing step, the pellet was re-suspended in TBS in order to obtain a semi-purified suspension of nuclei.

DNA profiles were examined using a flow cytometry station (MACSQuant Analyzer, Miltenyi). Histogram or density plots were arranged using the MACSQuant Digital software. For each sample, a minimum of 5 000 and a maximum of 15 000 particles were examined. Analyses were performed on five replicates for each sample. The percentage of the nuclei containing 2C and 4C DNA was calculated.

Hydrogen peroxide measurements

Extracellular H_2O_2 was determined by measuring the absorbance at 560 nm of the Fe^{3+}–xylenol orange complex according to Locato *et al.* (2008). The intracellular accumulation of H_2O_2 was also observed by using dihydrorhodamine (DHR) 123 (Sigma-Aldrich Italia, Milan, Italy) as a fluorescent probe according to Locato *et al.* (2008).

Determination of the reduced and oxidized forms of glutathione and ascorbate and the distribution of GSH between the nucleus and cytoplasm

Glutathione pool determinations were conducted on deproteinized samples, obtained from 0.3 g of cells homogenized with cold 5% metaphosphoric acid at 4 °C in a 1:2 ratio (w/v). After centrifugation at 20 000 *g* for 15 min, the supernatants were collected and used for the analysis of glutathione and ascorbate levels and redox states (reduced/reduced plus oxidized forms) according to de Pinto *et al.* (1999).

Aliquots of 20 µl of TBY-2 cells were stained with 5 µM CellTracker green 5-chloromethylfluorescein diacetate (CMFDA; Molecular Probes, Waltham, MA, USA) to detect GSH under a fluorescence microscope (DMLS, Leica, Wetzlar, Germany) with an excitation filter of 450–490 nm and a barrier filter of 510 nm as previously described by Markovic *et al.* (2007).

Enzyme assays

The cells were ground in liquid nitrogen and homogenized at 4 °C in extraction buffer [50 mm TRIS–HCl pH 7.8, 0.05% (w/v) cysteine, and 0.1% (w/v) BSA]. Homogenates were centrifuged at 20 000 *g* for 15 min. The supernatants were used for spectrophotometric analyses. The activities of ascorbate peroxidase (APX) (L-ASC: H_2O_2 oxidoreductase, EC 1.11.1.11), monodehydroascorbate reductase (MDHAR) (NADH: ASC-free radical oxidoreductase, EC 1.6.5.4), dehydroascorbate reductase (DHAR) (GSH: dehydroascorbate oxidoreductase, EC 1.8.5.1), GSH reductase (GR) (NADPH: GSH disulphide oxidoreductase, EC 1.6.4.2), and catalase (CAT–H_2O_2: H_2O_2 oxidoreductase, EC 1.11.1.6) were tested according to Locato *et al.* (2008). Protein measurement was performed according to Bradford (1976) using bovine serum albumin as a standard.

Confocal analysis

Cells were layered on glass-slides and quickly closed with cover slips. The slides were observed and images were obtained using a Nikon Eclipse TE2000-E inverted confocal microscope equipped with the EZ-C1 program (Nikon, Tokyo, Japan). Channel series acquisitions and related background subtraction were provided. Images (size: 512 × 512) were obtained with a ×40 objective (0.45 Numerical Aperture; Nikon). Z-stacks (30 steps for a step size of 0.40 µm) were acquired and deconvoluted in three dimensions (3D renders). PSD or TIFF-converted pictures were assembled by Adobe Photoshop 7.0 (Adobe Systems Inc., San Jose, CA), with no color/brightness adjustments.

Analysis of glutathionylated proteins

Western blot of total and nuclear proteins (50 and 35 µg per lane, respectively) extracted from TBY-2 cells was performed in non-reducing conditions and in the resence of *N*-ethyl maleimide (NEM) as mainly described by Hill *et al.* (2010). Extraction buffer contained 50 mM TRIS, 10 mM EDTA, 1 mM PMSF, 25 mM NEM pH 7.5 with HCl. Nuclear proteins were extracted by shaking the nuclear suspension at a medium-high speed for 30 min at 4 °C in a vortex with a tube attachment in the presence of 1% SDS. It was then centrifuged (10 min; 4 °C; 12 000 *g*), the supernatant was recovered, frozen in liquid nitrogen, and stored at –80 °C.

The total concentration of the extracted proteins was determined using a standard Bradford assay (Bradford, 1976). Briefly, a blocking step was performed in TBS-Tween with 5% (w/v) non-fat dry milk and 2.5 mM NEM for 1 h at room temperature, and probed against the anti-glutathione antibody (Virogen, Grater Boston, MA, USA) at a dilution of 1:1000 in TBS-Tween overnight at 4 °C, and secondary antibody, goat anti-mouse IgG (Bio-Rad, Hercules, CA, USA) conjugated to horseradish peroxidase, at 1:15000 in TBS-Tween for 1 h at room temperature. The detection procedure was performed using the Immuno-Star WesternC kit (Bio-Rad, Hercules, CA, USA). Image acquisition was made by ChemiDoc MP Imaging System (Bio-Rad, Hercules, CA, USA).

Determination of poly ADP-ribosylated proteins

The level of poly ADP-ribosylated proteins was measured by the immuno-detection of the poly ADP-ribose chains in protein extracts obtained from TBY-2 cells as fully described in Foyer *et al.* (2008). Equal amounts of cell proteins (0.5 mg) were spotted onto a Hybond C membrane which was pre-wetted with TBS buffer, and air-dried. The blocking step was performed in TBS with 5% (w/v) dried skimmed milk and 0.1% (v/v) Tween 20 with gentle agitation for 1 h. The membrane was then incubated for 1 h with anti-poly(ADP) ribose antibody (1:2500; Calbiochem, San Diego, CA, USA) and, after washing, detected with anti-rabbit IgG alkaline phosphate conjugate (Sigma-Aldrich, St Louis, MA, USA) as secondary antibody and alkaline phosphatase substrate BCIP-NBT (Sigma-Aldrich, St Louis, MA, USA) for 10–30 min until a clear signal was obtained. The reaction was stopped by washing the membrane repeatedly with ddH_2O. Image acquisition and densitometric analysis was made by ChemiDoc MP Imaging System and Software (Biorad, Hercules, CA, USA).

Statistical analysis

All the results were the means of at least three independent experiments. In each independent experiment, different cell cultures were used for ophiobolin A treatments and controls. The data were statistically analysed via Student *t* test using the Sigma Plot software or via ANOVA (Systat Software Inc., San Jose, CA, USA).

Results

The addition of ophiobolin A in the concentration range of 2–5 µM completely blocked the proliferation of TBY-2 cells (Fig. 1). However, the viability of the TBY-2 cells was

unaffected by these concentrations of the toxin (data not shown; see also Bury *et al.*, 2013). The growth and proliferation of TBY-2 had already ceased at 2 µM ophiobolin A (Fig. 1). Hence, this concentration was used to investigate the mechanism of ophiobolin A action on cell growth and proliferation.

No differences in the sizes of the TBY-2 cells were found after treatment with 2 µM ophiobolin A and the cells had similar elongation in the absence or presence of the inhibitor (see Supplementary Table S1 at *JXB* online). By contrast, the toxin decreased the mitotic index. The toxin-mediated inhibition of the mitotic index was evident after 4 h of treatment and progressively decreased over the following 24 h (Fig. 2). Cytofluorimetric analysis of nuclei isolated from ophiobolin A-treated tobacco cells at 24 h showed that fewer cells were undergoing mitosis. Moreover, there was a significantly larger number of cells at the S/G2 phases and a lower number in G1 after the ophiobolin A treatment (Fig. 3).

The level of total glutathione (GSH+GSSG) in the TBY-2 cells increased during proliferation, reaching a maximum level on the second day of culture (de Pinto *et al.*, 1999). After this point, the glutathione contents of the cells expressed on a fresh weight basis progressively decreased in control cells (Fig. 4). There was no decrease in total glutathione in ophiobolin A-treated cells after the second day of culture, the content of which remained at the maximum level for 48 h following the start of the treatment with the toxin (Fig. 4). The redox state of the glutathione pool (GSH/GSH+GSSG) did not change significantly in either the control or the treated cells over the course of the treatment (Fig. 4C). Indeed, the abundance of the oxidized form, glutathione disulphide (GSSG), relative to reduced glutathione (GSH) was unchanged and was maintained at very low levels following the application of the toxin. Therefore, the glutathione pool was higher in ophiobolin-treated cells compared with control cells (Fig. 4).

Total ascorbate (ASC+DHA) also increased during the TBY-2 cell culture, reaching maximum levels on the same day as the increase in the glutathione pool (data not shown, de Pinto *et al.*, 1999). Similar to glutathione, the total ascorbate content progressively decreased after the second day of culture in control cells (Fig.4B). When TBY-2 cells were treated with ophiobolin on the second day of culture, the total ascorbate level decreased with time. However, ascorbate levels remained higher than those of control cells over the course of the treatment (Fig. 4B). Moreover, ophiobolin A treatment led to an increase in the oxidized form of ascorbate (DHA). Therefore, after 120 h of ophiobolin treatment, the ascorbate redox state (ASC/ASC+DHA) had decreased (Fig. 4D).

In order to evaluate whether ophiobolin A changes the redox defence mechanisms of the tobacco cells, the levels of hydrogen peroxide and the activities of the ASC–GSH cycle enzymes and catalase (CAT) were measured (Fig. 5). Ophiobolin A treatment did not induce marked increases in

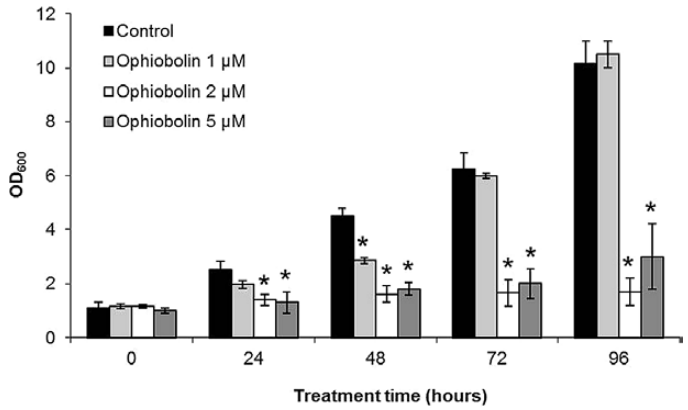

Fig. 1. Effect of ophiobolin A treatments on TBY-2 cell growth. Two days after the inoculation of TBY-2 cells in new culture medium (see the Materials and methods for details) the cells were treated with different concentrations of ophiobolin A. The growth of the cell culture was monitored measuring optical density (OD) at 600 nm over time. The reported values are the means of three independent experiments ±standard deviation. Asterisks indicate the values that are statistically different from the relative controls (Student's *t* test, $P < 0.05$).

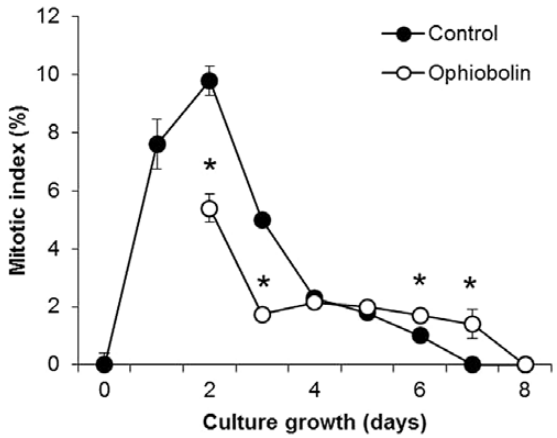

Fig. 2. Effect of ophiobolin A on mitotic index. The percentage of TBY-2 cells undergoing mitosis was evaluated at different time from inoculation day (day 0) to stationary phase (day 8). After 2 d of culture, cells were treated with 2 µM ophiobolin A. The first analysis of mitotic index was evaluated after 4 h (see the Materials and methods for details). The reported values are the means of three independent experiments ±standard deviation. Asterisks indicate the values that are statistically different from the relative controls (Student's *t* test, $P < 0.05$).

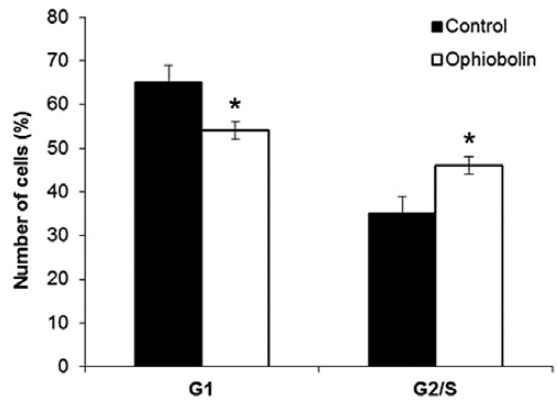

Fig. 3. Effect of ophiobolin A on the TBY-2 cell cycle. Nuclei were isolated from control and treated TBY-2 cells after 24 h of ophiobolin A treatment. The percentages of nuclear population in G1 versus G2/S phases were quantified cytofluorimetrically. The reported values are the means of three independent experiments ±standard deviation. Asterisks indicate the values that are statistically different from the relative controls (Student's *t* test, $P < 0.05$).

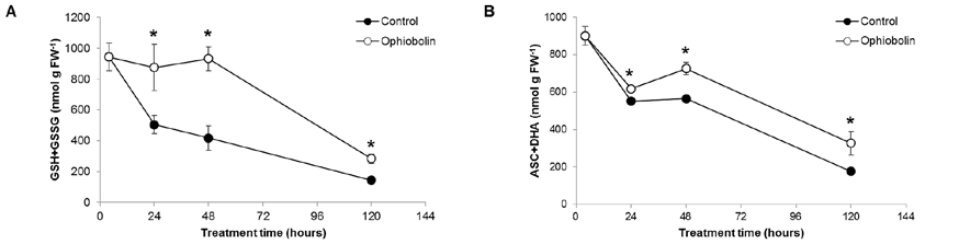

C

Treatment Time	Redox State (GSH / GSH+GSSG) 4 h	24 h	48 h	120 h
Control	0.98 ± 0.02	0.99 ± 0.01	0.99 ± 0.02	1.00 ± 0.02
Ophiobolin	0.97 ± 0.03	0.99 ± 0.02	0.98 ± 0.02	0.99 ± 0.03

D

Treatment Time	Redox State (ASC / ASC+DHA) 4 h	24 h	48 h	120 h
Control	0.78 ± 0.01	0.78 ± 0.05	0.79 ± 0.02	0.94 ± 0.04
Ophiobolin	0.72 ± 0.06	0.73 ± 0.06	0.74 ± 0.05	0.59 ± 0.15*

Fig. 4. Effect of ophiobolin A on the glutathione and ascorbate pools. Total glutathione (A) and total ascorbate (B) contents were quantified in control and ophiobolin A-treated cells. Cell glutathione and ascorbate redox state were determined as described in the Material and Methods and shown in (C) and (D), respectively. The reported values are the means of three independent experiments ±standard deviation. Asterisks indicate the values that are statistically different from the relative control (Student's *t* test, $P < 0.05$).

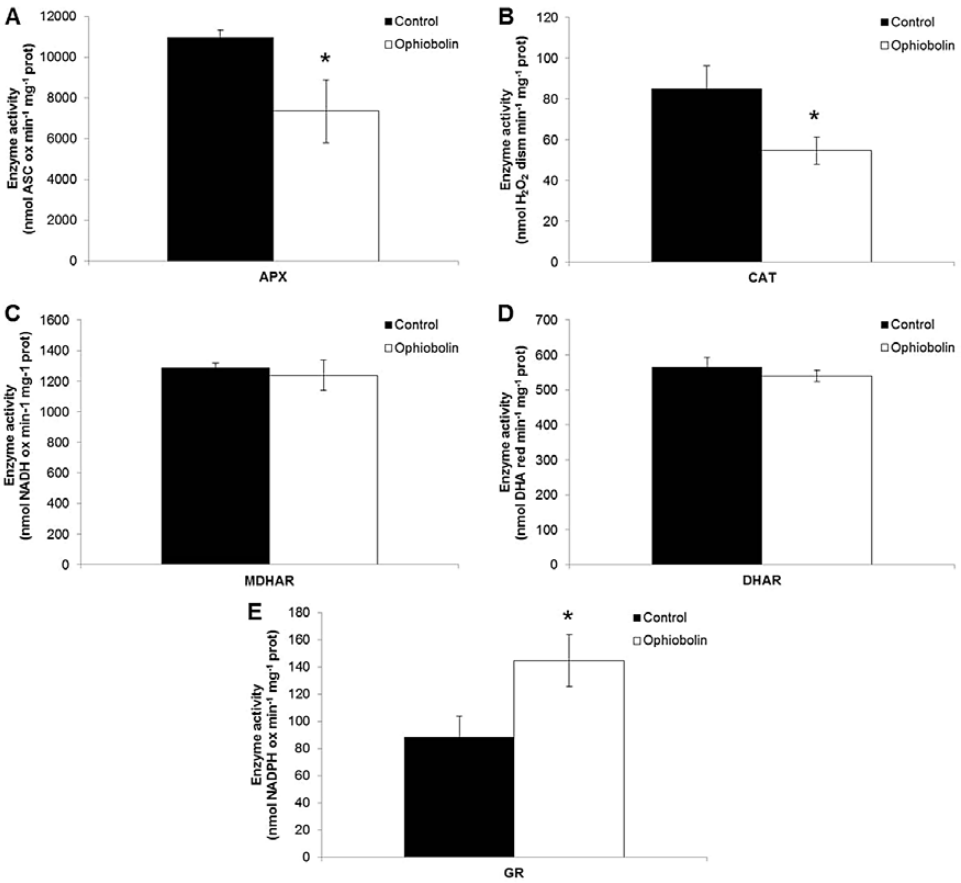

Fig. 5. Redox enzyme activities. Ascorbate peroxidase (A), catalase (B), monodehydroascorbate reductase (C), dehydroascorbate reductase (D) and glutathione reductase (E) activities were quantified at 24 h from the treatment in control and ophiobolin-treated cells. The reported values are the means of three independent experiments ±standard deviation. Asterisks indicate the values that are statistically different from the relative control (Student's *t* test, $P < 0.05$).

the cellular hydrogen peroxide content (data not shown, see also Bury et. al., 2013). The activity of ascorbate peroxidase (APX), an important plant enzyme involved in hydrogen peroxide scavenging, was decreased in ophiobolin A-treated cells 24 h after the start of the treatment (Fig. 5A). At the same time CAT activity had also decreased in the treated cells (Fig.5B). No changes in the activities of mono-dehydroascorbate reductase (MDHAR) and dehydroascorbate reductase (DHAR), the enzymes responsible for reducing to ASC the oxidized forms monodehydroascorbate and dehydroascorbate, respectively, were observed in cells treated with ophiobolin A (Fig. 5C, D). However, the toxin induced an increase in the activity of glutathione reductase (GR), the enzyme involved in the reduction of GSSG to GSH (Fig. 5D).

Early in the cell proliferation cycle, an increase in the proportion of GSH in the nucleus relative to the cytosol has been

reported in animal and plant cells (Pellny *et al.*, 2009; Vivancos *et al.*, 2010). GSH was found mainly in the nuclei of the TBY-2 cells during the first 2 d of cell culture growth, which corresponds to the period of maximum proliferative activity (Table 1; Fig. 6A). Thereafter, GSH was mainly detected in the cytoplasm of the TBY-2 cell, during the period when cells had stopped dividing (Fig. 6B, C; see Supplementary Fig. S2 at *JXB* online). At the stationary phase (8 d after the start of culture growth; Table 1) GSH was again mainly localized in the nuclei of the TBY-2 cells. Following ophiobolin A treatment, GSH was localized largely in the nuclei over the whole period of study (Fig. 6D, E, F). The intracellular distribution of GSH was clearly established by confocal studies (Fig. 7, see Supplementary Fig. S3 at *JXB* online).

Glutathione can interact with protein thiol groups in thiol–disulphide exchange and glutathionylation reactions. Protein glutathionylation is a post-translational protein modification that may be involved in the regulation of enzyme activities and cell signalling (Zaffagnini *et al.*, 2012). In order to determine whether ophiobolin A alters protein glutathionylation, the number and composition of the glutathionylated proteins were analysed in total cell and nuclear extracts of TBY-2 cells in the absence or presence of the toxin. A greater number of glutathionylated proteins were detected in the isolated nuclei than in the whole cell extracts (Fig. 8). More proteins were glutathionylated in ophiobolin A-treated cell extracts than in untreated controls. By contrast, the intensity of glutathionylated nuclear proteins and also the number of glutathionylated proteins was decreased as a result of ophiobolin treatment (Fig. 8).

The abundance of ADP-ribosylated proteins was also determined in the absence or presence of the toxin. The number of poly-ADP ribosylated proteins changed over the period of cell growth period with a maximum number observed at the beginning of the exponential phase (Fig. 9). The presence of ophiobolin A prevented this increase in the number of poly ADP-ribosylated proteins (Fig. 9).

Discussion

Cellular redox homeostasis is crucial to cell functions, particularly proliferation (de Pinto *et al.*, 1999; Pellny *et al.*, 2009; Vivancos *et al.*, 2010; Chiu and Dawes, 2012). Low molecular weight antioxidants such as ascorbate and glutathione are key components of this regulation in plant and animal cells (de Pinto *et al.*, 1999; Pellny *et al.*, 2009; Vivancos *et al.*, 2010; Chiu and Dawes, 2012). Ophiobolin A alters the metabolism of these two redox couples but in different ways. It appears that ophiobolin A does not increase ROS production or accumulation because the measured hydrogen peroxide levels were similar in the cells and in the culture medium, in the presence or absence of the toxin (Bury *et al.*, 2013). While the

Table 1. *Percentage of TBY-2 cells showing storage of GSH in nuclei*

Cells in the second day of cell cultures were treated with 2 μM ophiobolin A. The percentage of cells showing the presence of GSH within the nuclei was measured over time. The values are the means of three independent experiments ±standard deviation. In each experiment at least 500 cells were counted. Asterisks indicate the values that were statistically different form the relative control (Student's *t* test, $P < 0.05$).

	Treatment time (h)				
	4	24	48	72	144
Number of cells with nuclear GSH localization (%)					
Control	98±3	4±1	3±1	6±3	90±7
Ophiobolin A	97±3	95±5*	80±10*	85±12*	92±5

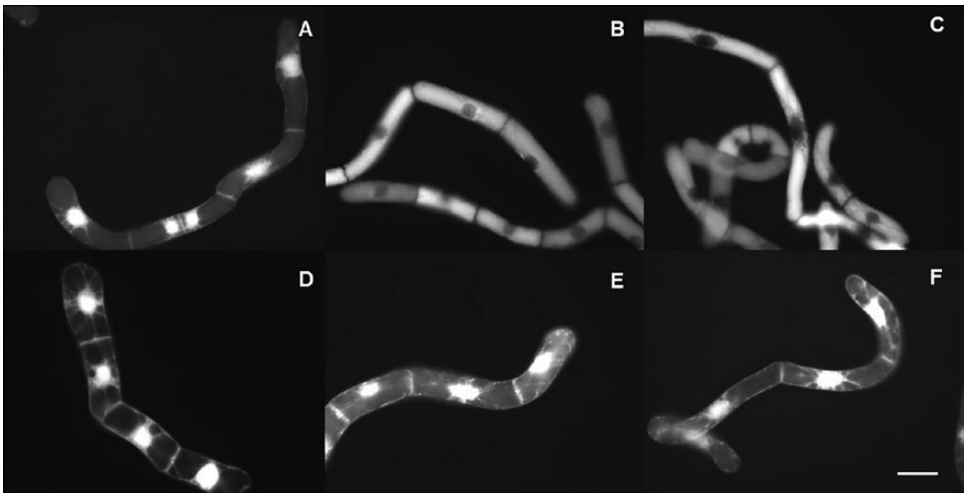

Fig. 6. GSH portioning in TBY-2 cells in control and ophiobolin A-treated TBY-2 cells. Representative images of TBY-2 cells after 4 h of treatment (A, control cells; D, ophiobolin-treated cells), after 48 h of treatment (B, control cells; E, ophiobolin-treated cells), and after 72 h of treatment (C, control cells; F, ophiobolin-treated cells).

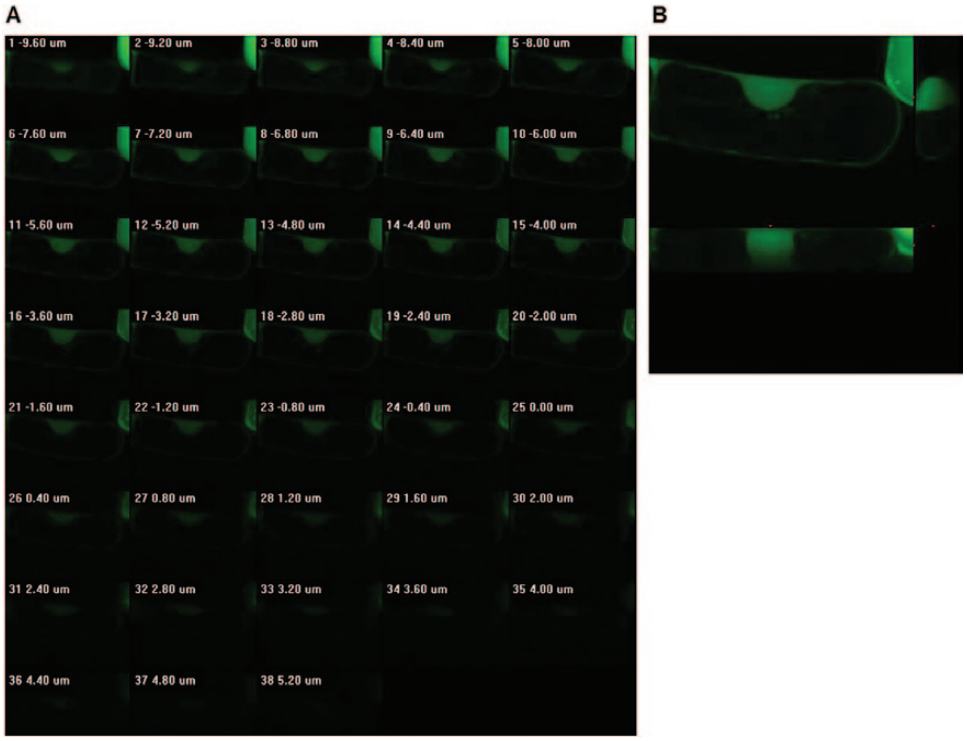

Fig. 7. Nuclear GSH localization. Cells were harvested at different times and layered onto glass-slides for EZ-C1 acquisition. Images were collected at 0.40 µm intervals with the 488 laser to create a *z*-stack. The *z*-stack render of an ophiobolin A-treated cell at 48 h from the treatment is displayed as a representative image. Note the specific fluorescence inside the nucleus as shown in the picture (magnification: ×400). (A representative gallery mode is shown in Supplementary Fig. S3 at *JXB* online).

possibility cannot be excluded that ROS production and/or levels might be changed at a sub-cellular level in specific localized cellular compartments in response to the presence of the toxin, APX and CAT activities were decreased in treated cells, again suggesting that the toxin did not increase ROS production. Similarly, there were no changes in the activities of the ASC recycling enzymes MDHAR and DHAR and a decrease in the ASC redox state was only significant after 120 h of treatment (Figs 4D, 5). However, in the presence of ophiobolin A, the cells increased their capacity to maintain the glutathione pool in the reduced state, since there was a significant increase in GR activity and the glutathione pool was largely present in the reduced form over the duration of the treatment and analysis (Figs 4C, 5). This observation suggests that GSH may be the main factor in the responses activated by the toxin.

Glutathione accumulates in the nuclei early in the cell cycle, where it fulfils key protective roles (García-Giménez *et al.*, 2013). Even in yeast, GSH protects the nucleus against oxidative damage, maintains genome stability, and facilitates transcriptional responses (Hatem *et al.*, 2014). The data presented here demonstrate that the presence of the toxin ophiobolin A leads to arrest of the cell cycle at the S/G2 phases in TBY-2 cell cultures and causes retention of GSH within the nucleus (Figs 3, 7; see Supplementary Fig. S3 at *JXB* online).

In an earlier study, it was demonstrated that the presence of ophiobolin A led to the programmed cell death (PCD) of TBY-2 cells when the toxin was added at concentrations of 10 µM or higher (Bury *et al.*, 2013). Ophiobolin A-triggered PCD was considered to be part of the overall defence response elicited by the presence of the toxin (Bury *et al.*, 2013). While lower ophiobolin A concentrations did not cause PCD, they led to a growth arrest in the tobacco cell cultures without adversely affecting cell viability (Bury *et al.*, 2013). The data presented here confirm that low concentrations of ophiobolin A block the cell cycle without affecting cell viability (Fig. 1). Moreover, ophiobolin A-triggered cell cycle arrest occurred before the cells enter mitosis, since mitotic index (i.e. the percentage of the dividing cells) was significantly decreased in the hours following the addition of ophiobolin A. The data presented here suggest that the toxin arrests the cell cycle at the S/G2 phases when the TBY-2 cells continue to grow and the nuclear chromosomes are duplicated before mitosis (Figs 2, 3). This inhibition occurred even though a large proportion of the cellular glutathione pool was localized in the nucleus, suggesting that GSH could not protect the cell cycle against ophiobolin A-mediated inhibition.

The total amount of glutathione increased progressively in the TBY-2 cells during the lag phase and at the beginning of exponential phase of growth, when mitotic activity of the cells cultures is higher (de Pinto *et al.*, 1999). The glutathione levels then decreased reaching the lowest values during the stationary phase of cell culture, in agreement with previous measurements made in *Arabidopsis* and tobacco (de Pinto *et al.*, 1999; Pellny *et al.*, 2009; Fig. 4A). The presence of ophiobolin A led to a change in the pattern of glutathione accumulation during cell proliferation (Fig. 4A). While glutathione levels increased in the TBY-2 cells during the lag phase and the exponential phase of growth, the toxin blocked the decrease in glutathione associated with the partitioning

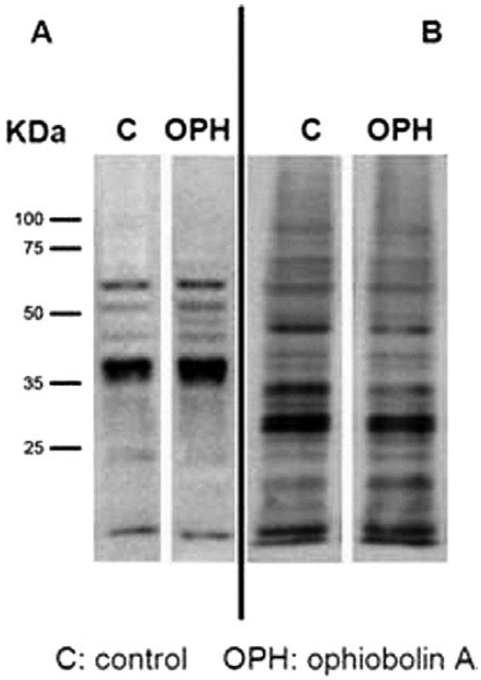

Fig. 8. Effects of ophiobolin A on glutathionylation of cellular and nuclear proteins. Representative Western blotting showing glutathionylated proteins extracted from whole cells (A) and nuclei (B) from control and 2 μM ophiobolin A-treated cells after 24 h of treatment. The same behaviour has been observed in another two independent experiments. See the Materials and methods for details. C, Control; OPH, ophiobolin A treatment.

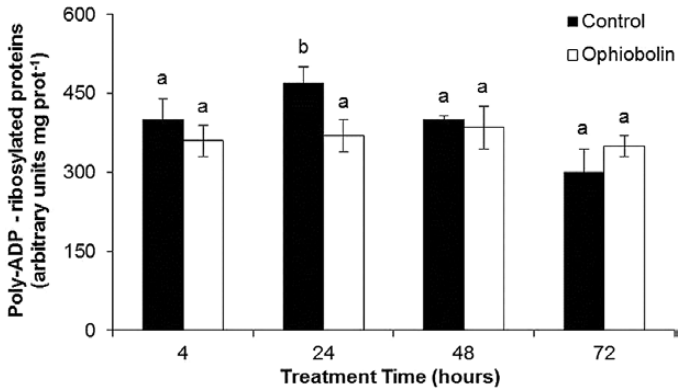

Fig. 9. Effects of ophiobolin A on poly ADP-ribosylated proteins. The level of poly-ADP-ribosylated proteins was measured in control and ophiobolin A-treated cells over time. The reported values are the means of three independent experiments ±standard deviation. An ANOVA test was performed in order to identify differences both over time and between treatments. Different letters indicate the values that are statistically different (P <0.05).

of the antioxidant between the daughter cells and also the re-distribution between nucleus and cytoplasm that is associated with the stationary phase. These data presented here not only confirm that GSH is localized in the nucleus during the early stages of cell proliferation in eukaryotic cells but they also provide further evidence that that nuclear localization of glutathione is determined by cell cycle progress because GSH is retained in the nucleus when the cell cycle is arrested at the S/G2 phases by ophiobolin A (Figs 6, 7; see Supplementary Fig. S3 at *JXB* online; Table 1). A more in-depth study is required to characterize the sub-cellular localization of GSH in the different cytoplasmic compartments in more detail. Nevertheless, our data provide evidence that at least part of the glutathione pool is present in the vacuole (see Supplementary Fig. S2 at *JXB* online). The vacuolar pool of glutathione is known to be important in regulating the redox state of the cytosol (Noctor *et al.*, 2014). The presence of glutathione in the vacuole could also be related to increased glutathione turnover as well as to the role of GSH in glutathione-*S*-transferase-dependent detoxification pathways. The vacuolar uptake of reactive and secondary metabolites that have been conjugated to GSH is important in degradation and detoxification reactions occurring in this cellular compartment (Foyer and Noctor, 2009; Noctor *et al.*, 2014).

The data presented here show that ophiobolin A leads to the arrest of the cell cycle at the S/G2 phases in TBY-2 cells but does not lead to changes in the glutathione redox state (Figs 3, 4, 6; Table 1). These data also suggest that the mechanisms that facilitate GSH transport and sequestration in nuclei are activated and deactivated in response to cell cycle checkpoints, as has been suggested in mammalian cells (Pallardó *et al.*, 2009). Alterations in the redox control of these checkpoints in animals have been linked to the abnormal proliferative activity of cancer cells, although the concept of a 'constitutive' decrease in cellular redox potential remains to be substantiated (Hoffman *et al.*, 2008). The pore-forming Bcl2 protein may be involved in GSH fluxes between the nucleus and cytoplasm in animals (Voehringer *et al.*, 1998). While Bcl2 proteins do not exist in plant genomes, Bcl-2-associated athanogenes such as BAG 6, which encodes for a calmodulin-dependent nuclear protein, might be involved in nuclear GSH transport (Vivancos *et al.*, 2010). While ophiobolin A is a calmodulin antagonist (Au *et al.*, 2000), the toxin did not prevent GSH accumulation in the nuclei during proliferation.

The data presented here indicate that the patterns of protein glutathionylation, particularly in the nuclei, were modified in the presence of ophiobolin A, suggesting that the toxin may alter GSH functions in the nuclei and cytosol during cell cycle progression (Fig. 8). The glutathionylation of nuclear proteins appears to be inhibited in the toxin-treated cells despite the presence of GSH in the nucleus (Fig. 8). The functions of glutathionylation are largely unknown (Klatt and Lamas, 2000) but this post-translational modification may protect proteins from oxidation or preserve the GSH pool in the presence of ophiobolin A. Glutathionylation of proteins may also be involved in the regulation of cell cycle progression. The glutathionylation of Jun, a component of the transcription factor AP-1 in mammalian cells, is involved in cell proliferation (Klatt *et al.*, 1999). This process regulates the ability of these proteins to bind DNA leading to changes in gene expression of cyclin D1 (Klatt *et al.*, 1999). Site-specific glutathionylation can also inhibit mitogen-activated protein kinases (Cross and Templeton, 2004). It has recently been demonstrated that histone H3 glutathionylation destabilizes the nucleosomal structure of mammalian cells, impairing cell cycle progression (García-Giménez *et al.*, 2013). It is possible that the alterations in ophiobolin A-induced protein

glutathionylation reported here (Fig. 8) might be linked to the regulation of cell cycle progression in a similar manner. The observed alteration in the activity of PARPs, which are enzymes transferring ADP-ribose groups from NAD^+ to nuclear proteins (Liang *et al.*, 2013; Robu *et al.*, 2013) might also suggest that nuclear metabolism is disrupted by sub-lethal concentrations of ophiobolin A. It has previously been observed that PARP activity increased during the proliferation of *Arabidopsis* cells and that the increase in PARP activity correlates with the cellular GSH content (Pellny *et al.*, 2009). PARP activity, measured by the abundance of poly-ADP ribosylated proteins, was also increased at the beginning of the exponential phase in the TBY-2 cells together with the increase in glutathione content. Ophiobolin A treatment decreased the abundance of poly-ADP ribosylated proteins in the TBY-2 cells (Fig. 9). PARPs are involved in DNA repair processes and their activation is required when cells are dividing (Pellny *et al.*, 2009). The observed decrease in the abundance of poly-ADP ribosylated proteins may, therefore, reflect the impaired replication of DNA in ophiobolin A-treated cells.

Taken together, the findings reported here not only demonstrate that ophiobolin A leads to cell cycle arrest at the S/G2 phases but they also provide further evidence of the underpinning cross-talk between glutathione and associated redox regulation in the control of cell cycle progression. The findings apply to the effects of the toxin in plant cells but it is likely that ophiobolin A has a similar mechanism of action in animal cells. Moreover, the action of the toxin provides further evidence linking nuclear glutathione to cell cycle control.

Supplementary data

Supplementary data can be found at *JXB* online.

Supplementary Table S1. TBY-2 cell size was monitored during the culture period under control and ophiobolin A treatment conditions.

Supplementary Fig. S1. Ophiobolin A structure.

Supplementary Fig. S2. A representative confocal image of TBY-2 control cells at 48 h after treatment.

Supplementary Fig. S3. A confocal study of control and ophiobolin A-treated cells was performed and a representative gallery mode (all the images in a single display) is reported for an ophiobolin A-treated cell at 48 h after treatment.

Acknowledgements

The authors thank Dr Maurizio Vurro, Istituto di Scienze delle Produzioni Alimentari, Consiglio Nazionale delle Ricerche, Bari, Italy, for supplying the culture filtrates of *D. gigantea*. The authors thank Professor Marisa Levi for her valued support in the cytofluorimetric analyses. The authors thank Dr Renato Alberto Rodrigues Pousada, Università degli Studi L'Aquila, Italy, for his scientific support in analysing confocal images. This research was carried out, in part, in the framework of Programme STAR, financially supported by UniNA and Compagnia di San Paolo, Napoli, Italy. A Micera was supported by the Italian Ministry of Health and Fondazione Roma (Italy). E Novo Uzal holds a JdC grant from MICINN (Spain) and is also indebted to the European Cooperation in Science and Technology Action FA1006-Plant Engine for a short-term scientific mission grant.

References

Au TK, Chick WSH, Leung PC. 2000. The biology of ophiobolins. *Life Science* **67,** 733–742.

Bradford MM. 1976. A rapid and sensitive method for the quantification of microgram quantities of protein utilizing the principle of protein–dye binding. *Analytical Biochemistry* **72,** 248–254.

Bury M, Novo-Uzal E, Andolfi A, *et al*. 2013. Ophiobolin A, a sesterterpenoid fungal phytotoxin, displays higher *in vitro* growth-inhibitory effects in mammalian than in plant cells and displays *in vivo* antitumor activity. *International Journal of Oncology* **43,** 573–585.

Canonica L, Fiecchi A, Galli Kienle M, Scala A. 1966. Isolation and constitution of cochliobolin B. *Tetrahedron Letters* **13,** 1329–1333.

Chiu J, Dawes IW. 2012. Redox control of cell proliferation. *Trends in Cell Biology* **22,** 592–601.

Cross JV, Templeton DJ. 2004. Oxidative stress inhibits MEKK1 by site-specific glutathionylation in the ATP-binding domain. *Biochemical Journal* **381,** 675–683.

de Pinto MC, Francis D, De Gara L. 1999. The redox state of the ascorbate-dehydroascorbate pair as a specific sensor of cell division in tobacco BY-2 cells. *Protoplasma* **209,** 90–97.

de Pinto MC, Locato V, De Gara L. 2012. Redox regulation in plant programmed cell death. Plant, *Cell and Environment* **35,** 234–244.

Dinneny JR, Long TA, Wang JY, Jung JW, Mace D, Pointer S, Barron C, Brady SM, Schiefelbein J, Benfey PN. 2008. Cell identity mediates the response of Arabidopsis roots to abiotic stress. *Science* **320,** 942–945.

Evidente A, Andolfi A, Cimmino A, Vurro M, Fracchiolla M, Charudattan R. 2006. Herbicidal potential of ophiobolins produced by *Drechslera gigantea*. *Journal of Agricultural and Food Chemistry* **54,** 1779–1783.

Foyer CH, Noctor G. 2009. Redox regulation in photosynthetic organisms: signalling, acclimation, and practical implications. *Antioxidants and Redox Signalling* **11,** 861–905.

Foyer CH, Pellny TK, Locato V, De Gara L. 2008. Analysis of redox relationships in the plant cell cycle: determinations of ascorbate, glutathione and poly (ADPribose) polymerase (PARP) in plant cell cultures. *Methods in Molecular Biology* **476,** 193–209.

Fried J, Perez AG, Clarkson BD. 1976. Flow cytofluorometric analysis of cell cycle distributions using propidium iodide. Properties of the method and mathematical analysis of the data. *The Journal of Cell Biology* **71,** 172–181.

García-Giménez JL, Markovic J, Dasí F, Queval G, Schnaubelt D, Foyer CH, Pallardó FV. 2013. Nuclear glutathione. *Biochimica et Biophysica Acta* **1830,** 3304–3316.

Hatem E, Berthonaud, V, Dardalhon M, Lagniel G, Baudouin-Cornu P, Huang M-E, Labarre J, Chédin S. 2014. Glutathione is essential to preserve nuclear function and cell survival under oxidative stress. *Free Radical Biology and Medicine* **67,** 103–114,

Hill BG, Ramana KV, Cai J, Bhatnagar A, Srivastava SK. 2010. Measurement and identification of *S*-glutathiolated proteins. *Methods in Enzymology* **473,** 179–197.

Hoffman A, Spetner LM, Burke M. 2008. Ramifications of a redox switch within a normal cell: its absence in a cancer cell. *Free Radical Biology and Medicine* **45,** 265–268.

Houot V, Etienne P, Petitot AS, Barbier S, Blein JP, Suty L. 2001. Hydrogen peroxide induces programmed cell death features in cultured tobacco BY-2 cells in a dose-dependent manner. *Journal of Experimental Botany* **52,** 1721–1730.

Jiang K, Ballinger T, Li D, Zhang S, Feldman L. 2006. A role for mitochondria in the establishment and maintenance of the maize root quiescent center. *Plant Physiology* **140,** 1118–1125.

Jiang K, Feldman LJ. 2005. Regulation of root apical meristem development. *Annual Review of Cell Development and Biology* **21,** 485–509.

Klatt P, Lamas S. 2000. Regulation of protein function by *S*-glutathiolation in response to oxidative and nitrosative stress. *European Journal of Biochemistry* **267,** 4928–4944.

Klatt P, Molina EP, De Lacoba MG, Padilla CA, Martinez-Galesteo E, Barcena JA, Lamas S. 1999. Redox regulation of c-Jun DNA binding by reversible *S*-glutathiolation. *FASEB Journal* **13,** 1481–1490.

Leung PC, Taylor WA, Wang JH, Tipton CL. 1984. Ophiobolin A. A natural product inhibitor of calmodulin. *Journal of Biological Chemistry* **259,** 2742–2747.

Leung PC, Taylor WA, Wang JH, Tipton CL. 1985. Role of calmodulin inhibition in the mode of action of ophiobolin A. *Plant Physiology* **77,** 303–308.

Liang YC, Hsu CY, Yao YL, Yang WM. 2013. PARP-2 regulates cell cycle-related genes through histone deacetylation and methylation independently of poly(ADP-ribosyl)ation. *Biochemical and Biophysics Research Communication* **431,** 58–64.

Locato V, de Pinto MC, De Gara L. 2009. Different involvement of the mitochondrial, plastidial, and cytosolic ascorbate–glutathione redox enzymes in heat shock responses. *Physiologia Plantarum* **135,** 296–306.

Locato V, Gadaleta C, De Gara L, de Pinto MC. 2008. Production of reactive species and modulation of antioxidant network in response to heat shock: a critical balance for cell fate. *Plant, Cell and Environment* **31,** 1606–1619.

Markovic J, Borrás C, Ortega A, Sastre J, Viña J, Pallardó FV. 2007. Glutathione is recruited into the nucleus in the early phases of cell proliferation. *Journal of Biological Chemistry* **282,** 20416–20424.

Markovic J, Mora NJ, Broseta AM, Gimeno A, de-la-Concepción N, Viña J, Pallardó FV. 2009. Nuclear GSH depletion impairs cell proliferation in 3T3 fibroblasts. *PLoS ONE* **29,** e6413.

Mauro F, Grasso A, Tolmach LJ. 1969. Variations in sulfhydryl, disulfide, and protein content during synchronous and asynchronous growth of HeLa cells. *Biophysics Journal* **9,** 1377–1397.

Menon SG, Goswami PC. 2007. A redox cycle within the cell cycle: ring in the old with the new. *Oncogene* **26,** 1101–1109.

Menon SG, Sarsour EH, Spitz DR, Higashikubo R, Sturm M, Zhang H, Goswami PC. 2003. Redox regulation of the G1 to S phase transition in the mouse embryo fibroblast cell cycle. *Cancer Research* **63,** 2109–2117.

Nagata T, Nemoto Y, Hasezawa S. 1992. Tobacco BY-2 cell line as the 'HeLa' cell biology of higher plants. *International Review of Cytology* **132,** 1–30.

Noctor G, Mhamdi A, Queval G, Foyer CH. 2014. Regulating the redox gatekeeper: vacuolar sequestration puts glutathione disulfide in its place. *Plant Physiology* . **163,** 665–671.

Nozoe S, Morisaki M, Tsuda K, Iitaka Y, Takahashi N, Tamura S, Ishibashi K, Shirasaka M. 1965. The structure of ophiobolin, a C_{25} terpenoid having a novel skeleton. *Journal of American Chemistry Society* **87,** 4968–4970.

Pallardó FV, Markovic J, García JL, Viña J. 2009. Role of nuclear glutathione as a key regulator of cell proliferation. *Molecular Aspects of Medicine* **30,** 77–85.

Pellny TK, Locato V, Vivancos PD, Markovic J, De Gara L, Pallardó FV, Foyer CH. 2009. Pyridine nucleotide cycling and control of intracellular redox state in relation to poly (ADP-ribose) polymerase activity and nuclear localization of glutathione during exponential growth of *Arabidopsis* cells in culture. *Molecular Plant* **2,** 442–456.

Robu M, Shah RG, Petitclerc N, Brind'amour J, Kandan-Kulangara F, Shah GM. 2013. Role of poly (ADP-ribose) polymerase-1 in the removal of UV-induced DNA lesions by nucleotide excision repair. *Proceedings of the National Academy of Sciences,USA* **110,** 1658–1663.

Vivancos PD, Dong Y, Ziegler K, Markovic J, Pallardo FV, Pellny TK, Verrier PJ, Foyer CH. 2010. Recruitment of glutathione into the nucleus during cell proliferation adjusts whole-cell redox homeostasis in *Arabidopsis thaliana* and lowers the oxidative defence shield. *The Plant Journal* **64,** 825–838.

Voehringer DW, McConkey DJ, McDonnell TJ, Brisbay S, Meyn RE. 1998. Bcl-2 expression causes redistribution of glutathione to the nucleus. *Proceedings of the National Academy of Sciences, USA* **95,** 2956–2960.

Zaffagnini M, Bedhomme M, Lemaire SD, Trost P. 2012. The emerging roles of protein glutathionylation in chloroplasts. *Plant Science* **186,** 86–96.